processes

MDPI

Article

Continuous DeNOx Technology for Improved Flexibility and Reliability of 1000 MW Coal-Fired Power Plants: Engineering Design, Optimization, and Environmental Benefits

Xinrong Yan [1,2], Jianle He [2,*], Dong Guo [2], Yang Zhang [2], Xiwei Ke [3], Hongliang Xiao [3], Chenghang Zheng [1,*] and Xiang Gao [1]

[1] State Key Laboratory of Clean Energy Utilization, State Environmental Protection Center for Coal-Fired Air Pollution Control, Zhejiang University, Hangzhou 310027, China
[2] Huadian Electric Power Research Institute Co., Ltd., Hangzhou 310013, China
[3] State Key Laboratory of Power Systems, Department of Energy and Power Engineering, Tsinghua University, Beijing 100089, China; honglx0805@gmail.com (H.X.)
* Correspondence: hejianle5@163.com (J.H.); zhengch2003@zju.edu.cn (C.Z.)

Abstract: This study endeavors to enhance the operational efficiency of extant coal-fired power plants to mitigate the adverse environmental impact intrinsic to the prevalent utilization of coal-fired power generation, which is particularly dominant in China. It focuses on the assessment and optimization of continuous denitrification systems tailored for a 1000 MW ultra-supercritical pulverized coal boiler. The extant denitrification framework encounters challenges during startup phases owing to diminished selective catalytic reduction (SCR) inlet flue gas temperatures. To ameliorate this, three retrofit schemes were scrutinized: direct mixing of high-temperature flue gas, bypass flue gas mixing, and high-temperature flue gas mixing with cold air. Each option underwent meticulous thermodynamic computations and comprehensive cost analyses. The findings elucidated that bypass flue gas mixing, involving the extraction and blending of high-temperature flue gas, emerged as the most financially prudent and practical recourse. This scheme optimizes fuel combustion heat utilization, significantly curtails fuel consumption, and fosters efficient internal heat transfer mechanisms within the boiler. The evaluation process meticulously considered safety parameters and equipment longevity. The insights derived from this investigation offer valuable guidance for implementing continuous denitrification system retrofits in industrial coal-fired power plants.

Keywords: continuous DeNOx technology; coal-fired power plants; SCR; environmental performance

Citation: Yan, X.; He, J.; Guo, D.; Zhang, Y.; Ke, X.; Xiao, H.; Zheng, C.; Gao, X. Continuous DeNOx Technology for Improved Flexibility and Reliability of 1000 MW Coal-Fired Power Plants: Engineering Design, Optimization, and Environmental Benefits. *Processes* **2024**, *12*, 56. https://doi.org/10.3390/pr12010056

Academic Editors: Blaž Likozar and Ye Huang

Received: 27 October 2023
Revised: 29 November 2023
Accepted: 20 December 2023
Published: 26 December 2023

1. Introduction

Energy and environmental issues are closely related to social security and sustainable economic development. In order to address the global challenge of climate change, China announced in 2020 its ambitious goals of reaching peak carbon emissions by 2030 and achieving carbon neutrality by 2060 [1–6]. Currently, coal-fired power generation holds the dominant position in China, necessitating a transformation of the country's power system [7,8]. It is necessary to deepen the reform of the electricity market and guide and regulate power generation companies to develop toward higher efficiency and cleaner practices [9–11]. This will help in shifting the future focus of power development toward the utilization of non-fossil energy sources, thus advancing low-carbon transformation [12–15]. Consequently, the future development focus of existing coal-fired power plants will shift from increasing installed capacity to enhancing the flexibility and reliability of the current units.

With the deceleration of electricity consumption growth and the proliferation of coal-fired generating units, these units are anticipated to serve the purposes of deep load

modulation and standby to accommodate the rapid expansion of non-fossil energy generation [16]. Consequently, the operational hours of thermal power generation equipment are expected to further diminish. In the near future, extended operation at reduced loads and frequent start–stop cycles of coal-fired units will become standard practice [17–21]. Nonetheless, both deep load modulation and startup processes entail the risk of non-operational denitrification, which can result in excessive NOx emissions from the units.

Xie et al. [22] conducted thermal state tests on a 300 MW CFB boiler after implementing flue gas recirculation. The analysis revealed significant changes in parameters such as emissions, bed temperature, and separator inlet temperature. The results demonstrated the effectiveness of flue gas recirculation in reducing NOx emissions during startup and normal operation. Taler et al. [23] examined the flexibility needs of power systems involving thermal units, focusing on short startup times, SCR performance, and emissions analysis. Shen et al. [24] conducted research on CFB boilers, utilizing the CFD method to analyze flow field changes and pollutant emissions (SO_2 and NO) during thermal startup. The findings provide valuable insights for understanding CFB boiler startup and operation. Boiler emissions must remain within the specified limits during low-load operation, startup, shutdown, and under different load conditions. The implementation of continuous flue gas denitrification throughout all operational phases, including startup and shutdown, will progressively become an established environmental mandate [25]. During the startup phase, the failure to activate the denitrification system leads to the emission of excessive NOx, potentially resulting in environmental penalties and even hindering the unit from initiating the startup process [23,24,26–31]. Previous research suggests the challenge of controlling pollutant emissions during the start–stop stage. However, previous studies often overlook reducing pollutant emissions from the system's thermal equilibrium standpoint, whereas this study focuses on minimizing emissions by effectively utilizing system heat.

During the startup process of coal-fired units, the outlet concentration of NOx in the furnace rises sharply above the limits when coal powder is introduced. However, at this stage, the temperature of the selective catalytic reduction (SCR) inlet flue gas remains below 200 °C, significantly deviating from the operational requirements of the denitrification equipment. To ensure the smooth startup of the boiler and maintain the average concentration of NOx emissions from the furnace outlet within acceptable limits during the startup phase, power plants employ the substitution of fuel oil for coal powder combustion until the SCR inlet flue gas temperature reaches the requisite conditions for denitrification operation. Only then is coal powder combustion initiated. However, this practice poses challenges to the regular fuel powder injection for the boiler and extends the duration of oil-fired operation during the startup phase. It leads to increased operating costs during startup and has detrimental effects on downstream environmental protection equipment, including catalyst deactivation, dust collector bag clogging, and risks associated with desulfurization slurry poisoning.

The primary goal of this study is to evaluate the viability of integrating continuous flue gas denitrification retrofits within coal-fired power generation units. Specifically, the research zeroes in on the economic dimensions of this retrofitting procedure. The overarching aim is to augment the capability of coal-fired power units, enabling them to seamlessly integrate renewable energy sources. Simultaneously, the study aims to fortify technological capabilities to align with increasingly stringent environmental regulations. Paramount in this pursuit is ensuring a secure, clean, and reliably stable operation within the power system.

2. Overview of Pulverized Coal Boiler

2.1. Boiler Hourmenon

This study focuses on an 1000 MW ultra-supercritical pulverized coal boiler that utilizes a single-furnace tower arrangement. The rear flue gas outlet is equipped with two selective catalytic reduction (SCR) reaction devices, each of which is accompanied by a rotary air preheater positioned below it. Figure 1 provides a plan view, while Figure 2

offers a side view of the comprehensive layout of the boiler. The overall dimensions of the boiler are as follows: furnace width of 20,760 mm, furnace depth of 20,760 mm, lower header elevation of the water-cooled wall at 7500 mm, furnace top pipe center elevation at 121,500 mm, and top elevation of the large plate beam at 131,400 mm. During the startup of the unit, when the boiler load falls below 30% of the boiler maximum continuous rating (BMCR), the medium from the outlet of the evaporator heating surface gathers in a collector box after passing through the water-cooled wall outlet. Subsequently, it is conveyed to the steam–water separator through four pipes for separation into steam and water. The upper part of the boiler features a sequential arrangement of the low-temperature superheater, the low-temperature section of the high-temperature reheat, the high-temperature superheater, the high-temperature section of the high-temperature reheat, the low-temperature reheat, and the economizer, all aligned along the flue gas flow direction. The heating surfaces in the upper part of the boiler are horizontally arranged, and the through-wall structure takes the form of a fully sealed metal enclosure.

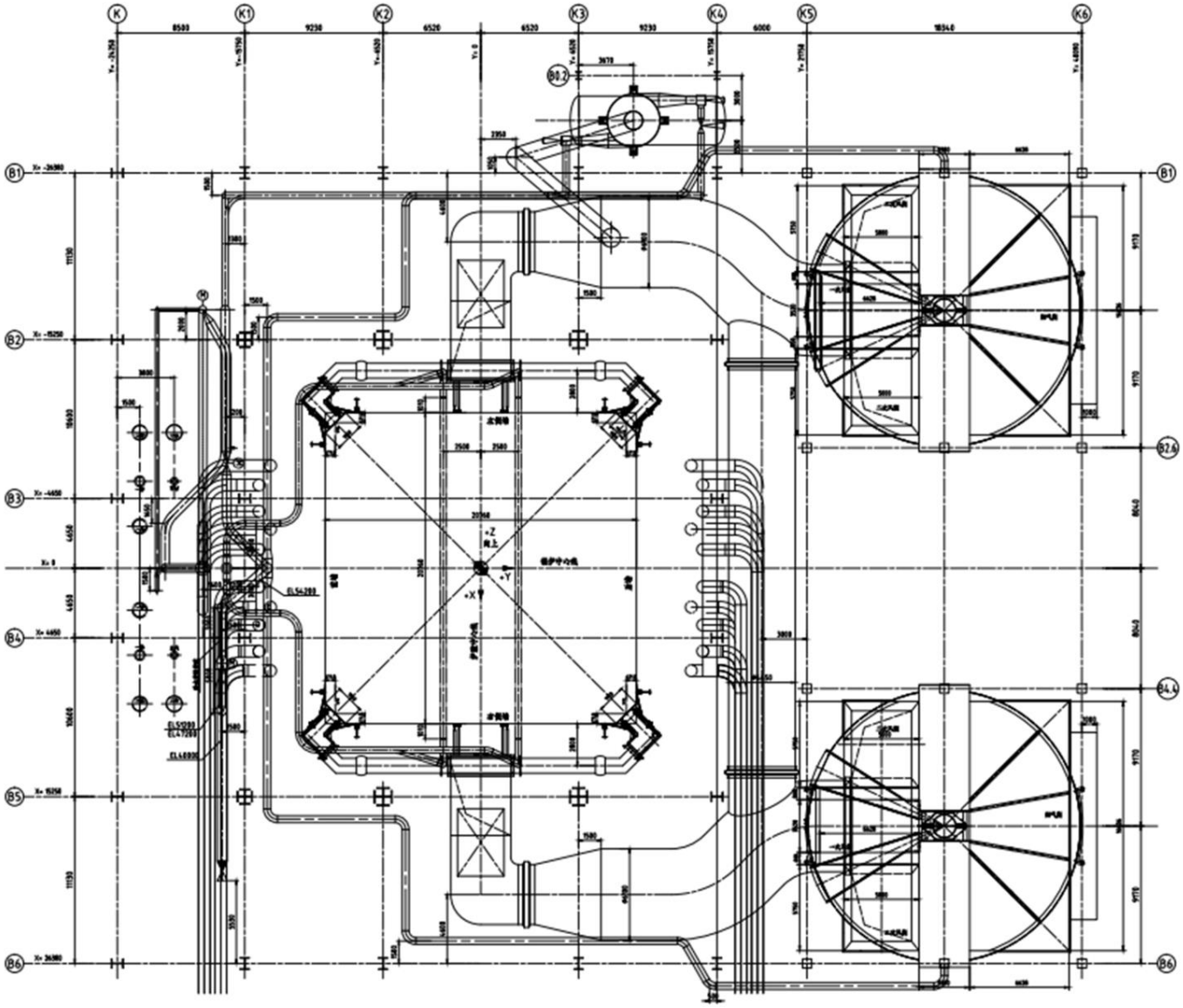

Figure 1. General layout plan (vertical view) of the boiler.

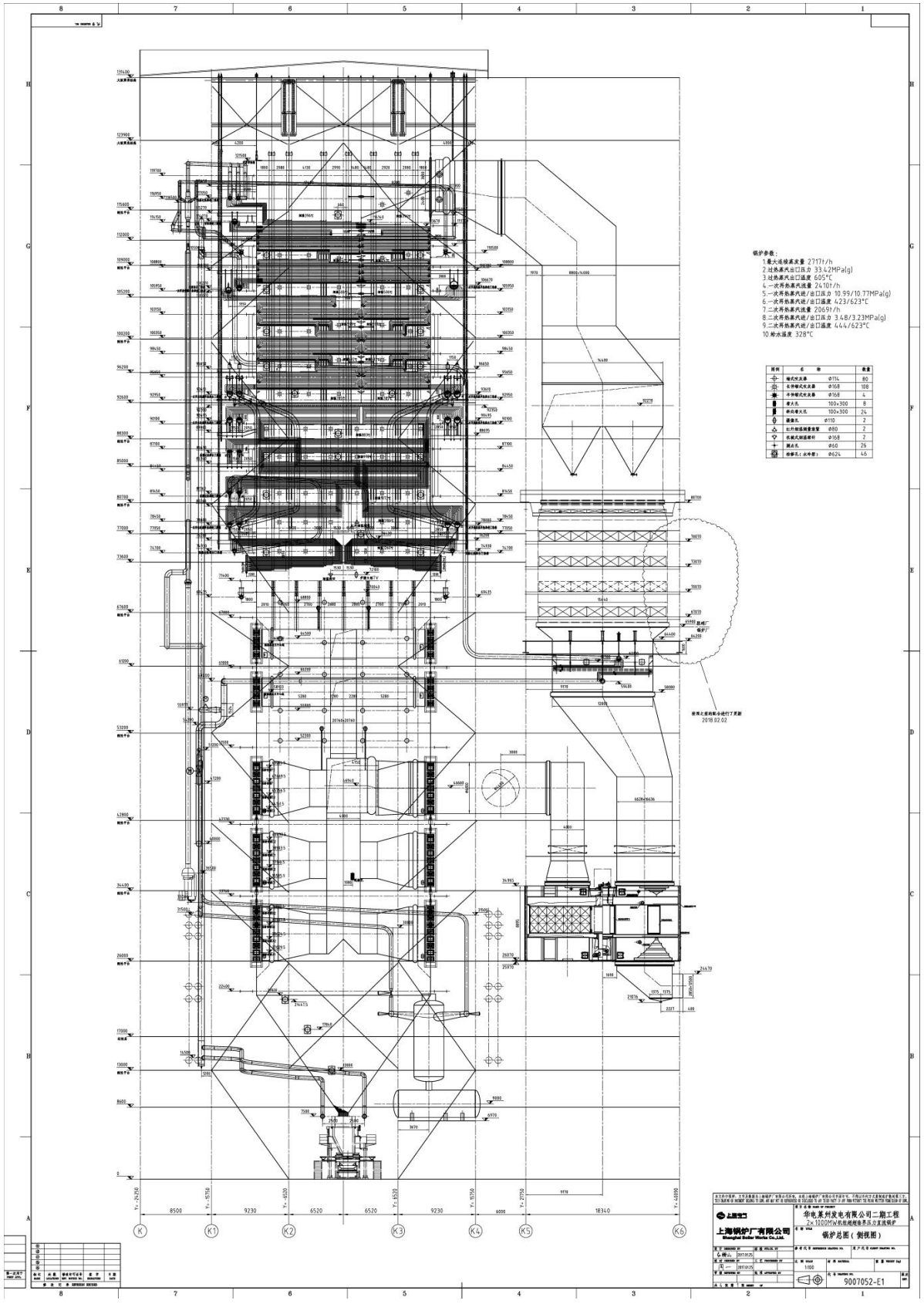

Figure 2. General layout plan (end view) of the boiler.

The boiler's combustion system is designed as a medium-speed pulverized-coal positive-pressure direct-blowing pulverization system. It is equipped with six coal mills, and each coal mill is connected to four coal powder pipes that lead to the four corners of the furnace. Outside the furnace, there is a coal powder distribution device. Each pipe is divided into two pipes using a coal powder distributor, and these pipes are connected to two adjacent primary air nozzles. Forty-eight tangentially fired burners are arranged in twelve layers at the lower corners of the furnace, with two coal powder nozzles per layer, enabling circular combustion in the furnace corners. The entire boiler is vertically divided into five groups of burners. The upper two groups are dedicated to secondary air distribution and consist of four layers with four air chambers each. The lower three groups consist of coal powder burners, each group having four layers of coal powder nozzles, resulting in a total of 48 burner nozzles. Each of the three groups of coal powder burners is equipped with two layers of retractable mechanical atomizing oil guns and six layers of fuel oil nozzles, resulting in a total of 24 oil guns in the burner windbox.

The upper part of the boiler is linked to the inlet flue of the denitration device and the ash hopper at the outlet of the economizer. The flue descends, and its vertical load is directly supported and suspended on the plane of the furnace roof steel frame. At the economizer outlet, the flue is divided into two paths. Each path passes through its respective closing baffle before entering the denitration device and then proceeds to two four-compartment rotary air preheaters. The boiler is equipped with SCR denitration equipment in synchronization with the economizer's outlet flue. A wind-cooled dry slag removal device is used to discharge solid slag from the bottom of the boiler furnace.

2.1.1. Design Coal

The designated coal type was Inner Mongolia bituminous coal. The ultimate and proximate analysis data are available in Table 1.

Table 1. Ultimate and proximate analyses of the design fuel for the 1000 MW ultra-supercritical pulverized coal boiler.

Item	Symbol	Unit	Value
1. Ultimate analysis			
Carbon	C_{ar}	%	51.09
Hydrogen	H_{ar}	%	3.45
Oxygen	O_{ar}	%	6.14
Nitrogen	N_{ar}	%	0.77
Sulfur	S_{ar}	%	0.70
2. Proximate analysis			
Moisture	M_{ar}	%	16.1
Moisture	M_{daf}	%	7.81
Ash	A_{ar}	%	21.75
Ash	V_{daf}	%	37.96

Note: subscript daf: air-dry and ash-free; subscript ar: as-received base.

2.1.2. Boiler Operating Conditions

The boiler operates under the following conditions:

It functions as a base load unit and participates in peak shaving.

It utilizes the designed coal type to ensure that the minimum stable combustion load is no more than 30% of its BMCR and maintains 100% automation input rate above this load range.

It adopts micro-oil ignition with small oil guns and retains large oil guns for combustion assistance. The modified configuration consists of 8 small oil guns with a capacity of 120 kg/h each and 24 large oil guns with a capacity of 450 kg/h each.

It adjusts the load change rate according to the following criteria: from 50% to 100% of BMCR: at least ±5% of BMCR per minute; from 30% to 50% of BMCR: at least ±3% of

BMCR per minute; below 30% of B-MCR: at least ±2% of B-MCR per minute; load step change: more than 10% of the turbine rated power per minute.

It controls the temperature range of the superheater and reheater to ensure stable operation within the following parameters: superheated steam temperature: 30–100% of B-MCR with a deviation within ±5 °C; reheat steam temperature: 50–100% of B-MCR.

It aligns the startup time from ignition to full-load operation with the turbine and typically meets the following requirements: cold start: 5–6 h; warm start: 2–3 h; hot start: 1–1.5 h.; very hot start: less than 1 h. Furthermore, the time from boiler ignition to turbine synchronization should meet the following requirements: cold start: 3.5 h; warm start: 2 h; hot start: 1 h; very hot start: 0.5 h.

2.1.3. Main Thermal Parameters of the Boiler

The main thermal parameters of the boiler are shown in Table 2.

Table 2. Main thermal parameters of the boiler.

No.	Name	Unit	BMCR	BRL	THA	75%THA	50%THA	30%BMCR
1	Superheated steam flow	t/h	2717	2638	2557	1839	1188	815
2	Outlet pressure of superheated steam	MPa·g	33.42	32.52	31.62	23.28	15.35	10.63
3	Outlet temperature of superheated steam	°C	605	605	605	605	605	605
4	Primary reheated steam flow	t/h	2410	2340	2277	1668	1097	760
5	Inlet pressure of primary reheated steam	MPa·g	10.99	10.67	10.4	7.68	5.07	3.51
6	Inlet temperature of primary reheated steam	°C	423	423	424	428	433	436
7	Outlet pressure of primary reheated steam	MPa·g	10.77	10.45	10.19	7.51	4.96	3.43
8	Outlet temperature of primary reheated steam	°C	623	623	623	623	623	608
9	Secondary reheated steam flow	t/h	2069	2006	1961	1460	978	687
10	Inlet pressure of secondary reheated steam	MPa·g	3.48	3.37	3.3	2.44	1.62	1.11
11	Inlet temperature of secondary reheated steam	°C	444	444	445	448	452	455
12	Outlet pressure of secondary reheated steam	MPa·g	3.23	3.12	3.06	2.26	1.48	1.01
13	Outlet temperature of secondary reheated steam	°C	623	623	623	623	623	605
14	Temperature of feeding water	°C	328	326	324	303	276	254
15	Inlet steam pressure of economizer	MPa·g	37.42	36.29	35.17	25.12	16.11	10.99

2.1.4. Brief Introduction to the Boiler System

The boiler's startup system features an integrated steam–water separator along with a startup recirculation pump. Additionally, it is equipped with a straightforward drainage system comprising an atmospheric expansion tank and a collection tank. The feedwater entering the economizer is simultaneously provided by both the recirculation pump and the feedwater pump.

The main feedwater pipe of the boiler enters the front of the boiler and traverses a main check valve and an electric main gate valve. It subsequently divides into two branches, with each branch connected to an inlet header of a two-stage economizer (one side only). Upon traversing the two-stage economizer and the main economizer, the pipes come together at the outlet header of the main economizer. The outlet pipes from both sides of the economizer merge at the front of the furnace and form a descending pipe that connects the top and bottom of the inlet header located at the bottom of the water-cooled wall.

The superheater system comprises two levels of primary heating surfaces. The first level encompasses suspended tubes, partitions, and low-temperature superheaters. On the other hand, the second level consists of high-temperature superheaters. The primary reheater is divided into two levels: the primary reheater low-temperature section and the primary reheater high-temperature section. The low-temperature section of the primary reheater is arranged in the upper front flue gas path. The cold section of the high-temperature section is located between the low-temperature superheater and the high-temperature superheater, while the hot section of the high-temperature section is positioned between the high-temperature superheater and the low-temperature reheater. The low-temperature section of the primary reheater is arranged between the high-temperature reheater and the economizer. The secondary reheater follows a similar arrangement to the primary reheater.

2.1.5. SCR System

The SCR process, utilizing a honeycomb catalyst configuration, was adopted for selective catalytic reduction. Urea hydrolysis was employed as the reducing agent for denitrification, with the flue gas temperature controlled within the range of 300 to 420 °C. Each furnace is equipped with two SCR reactors featuring air distribution devices at the reactor inlets and deflector plates in the flue gas ducts.

3. Analysis of the Current Operating Condition of the Unit

3.1. Startup Condition

The data in Figure 3 illustrate the SCR inlet flue gas temperature and NOx emission concentration curves during the startup phase of a 1000 MW coal-fired plant. It is crucial to maintain the system's total energy constant throughout the process, ensuring equilibrium between coal-derived input energy and outputs like heat, electricity, and losses (e.g., friction and radiation). The heat transfer mechanism involves conduction, convection, and radiation from coal to the boiler tubes, steam, turbine, and generator. Pulverized coal injection significantly elevates NOx emissions at the furnace outlet, surpassing standard limits swiftly. Nonetheless, the SCR inlet flue gas temperature (<300 °C) remains below the optimal operational range of the denitrification system (from 300 °C to 420 °C). This significant divergence between the SCR inlet flue gas temperature and the denitrification system's working temperature poses a challenge to effective DeNOx system functioning, necessitating a flue gas temperature increase. This investigation explores three potential schemes to elevate the SCR inlet flue gas temperature in a 1000 MW coal-fired power plant.

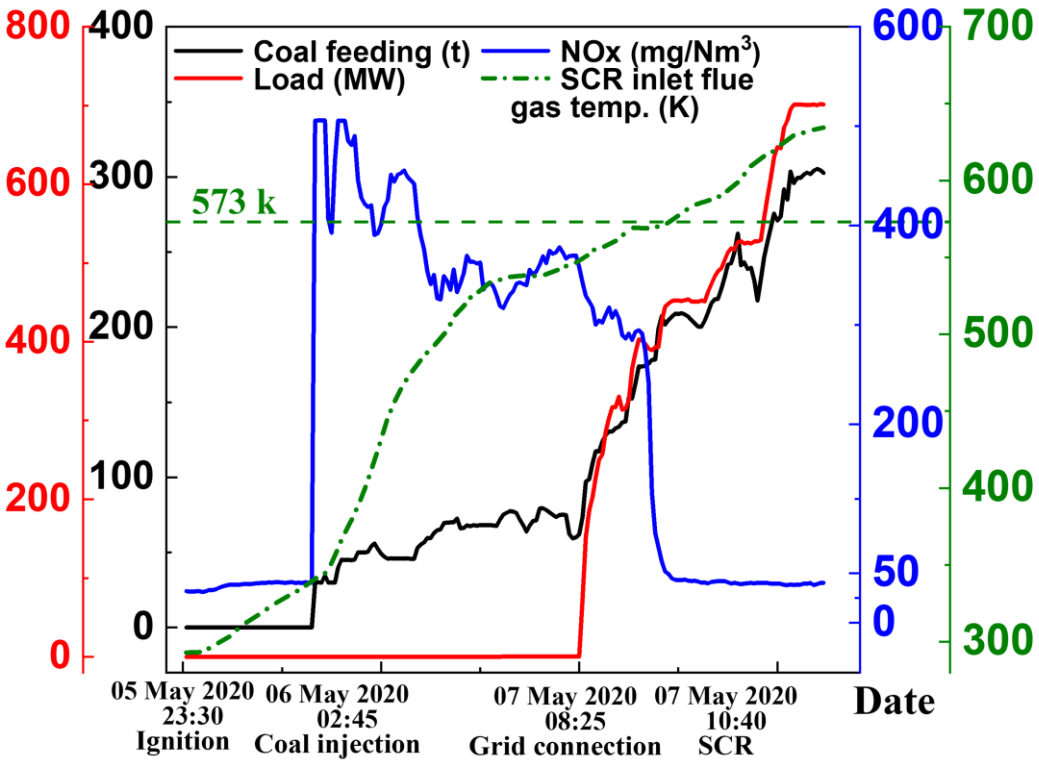

Figure 3. Profiles of various parameters during the startup process of a 1000 MW coal-fired power plant.

3.1.1. Analysis of Heating System

During the ignition and warm-up stage of the boiler, a significant portion of the heat generated from fuel combustion is dedicated to elevating the temperature of the furnace water. A higher initial temperature of the furnace water leads to reduced heat absorption by the water-cooled walls, resulting in a more rapid temperature increase within the furnace

and decreased pressure for retrofitting the continuous flue gas denitrification system during the operational period.

The utilization of thermodynamic principles and mathematical formulations enables the generation of the curves in Figure 4. This relationship is mathematically expressed as:

$$\Delta E = Q - W,$$

where ΔE signifies the internal energy change of the system, Q denotes the heat input to the system, and W represents the work executed by the system. Here, the heat supplied to the system corresponds to the heat content from the flue gas, while the system's work is the compression work applied to the cold air. Figure 4 delineates the temperature ascent curve within the water circuit preceding boiler ignition. After heating in the deaerator and multiple high-pressure heater stages, the primary feedwater undergoes blending with circulating water from the pressurized storage tank before being directed toward the economizer. The illustration shows that before the auxiliary heating system commences, the deaerator outlet sustains a consistent temperature of roughly 150 °C. Concurrently, the storage tank's water temperature registers around 84 °C, while the primary economizer's inlet water temperature hovers at approximately 108.2 °C. At 16:55, the auxiliary heating system attains peak output. During this interval, the main feedwater temperature (post-economizer) peaks at about 270 °C, whereas the storage tank's water temperature reaches approximately 133.4 °C, and the primary economizer's inlet water temperature climbs to around 168.4 °C. Initial estimates suggest that absent the auxiliary heating system operation, the furnace water temperature via the deaerator could only reach roughly 90 °C. However, with the auxiliary heating system functioning optimally, the furnace water temperature elevates within the range of 150–180 °C.

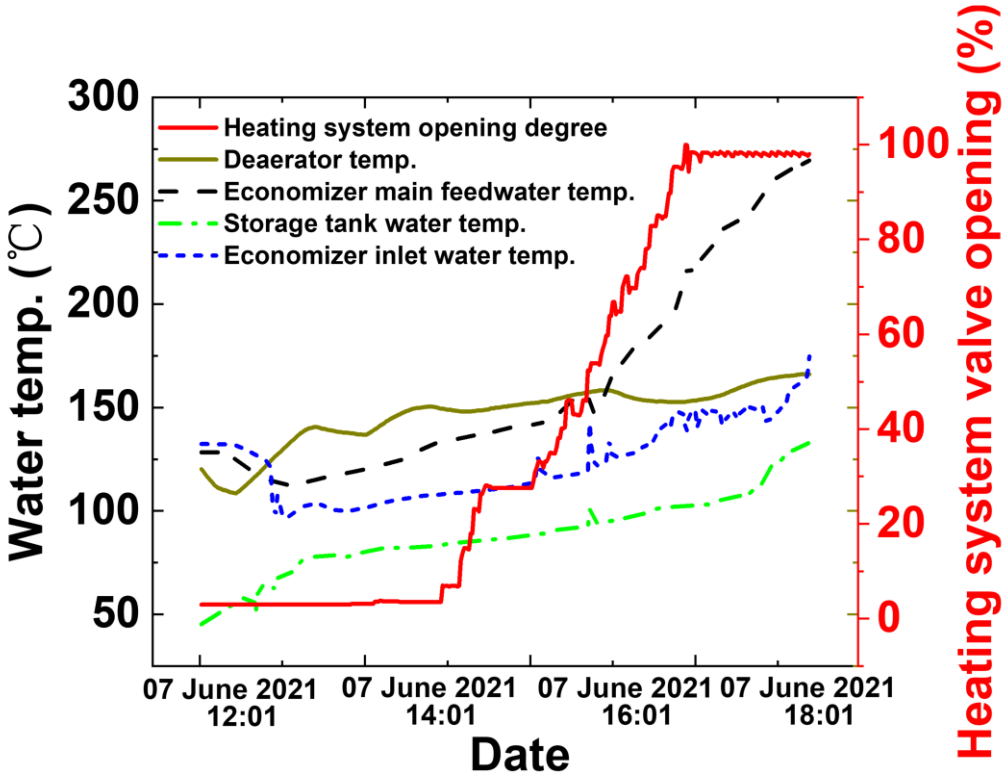

Figure 4. Curve of temperature rise in the water side before ignition.

3.1.2. SCR Inlet Flue Gas Temperature

The inlet flue gas temperature of the SCR system was determined using a grid method and compared with the readings from the dial display. The flue gas temperature distribution

during three different time periods (120 °C, 150 °C, and 180 °C) was measured using the grid method and is illustrated in Figure 5. The measured average values obtained from the grid method during these time periods were found to be 120.0 °C, 148.1 °C, and 180.0 °C, respectively, demonstrating a close agreement with the dial display values. Moreover, the flue gas temperature distribution at the inlet section of the SCR exhibited a relatively uniform pattern.

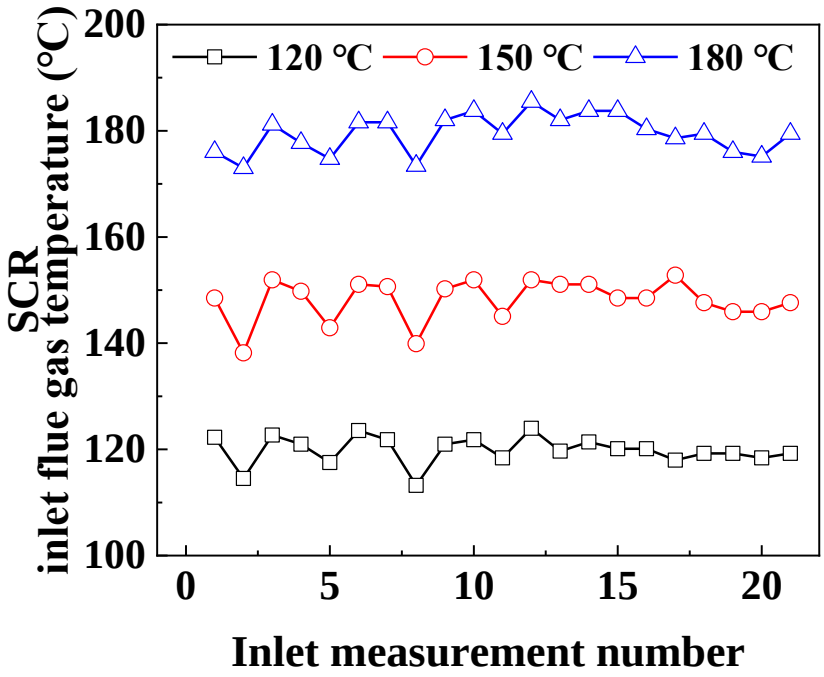

Figure 5. SCR inlet flue temperature distribution.

4. Solution Analysis

Currently, mature denitrification technologies for wide-load operations, including staged economizers, hot water recirculation, bypass of economizers (water side), and bypass of flue gas ducts (gas side), primarily rely on internal heat transfer within the unit to raise the inlet flue gas temperature of the selective catalytic reduction (SCR) system to the permissible denitrification temperature. However, during the startup phase of the unit, the furnace lacks a suitable temperature range to achieve the required SCR inlet flue gas temperature through internal heat transfer. Consequently, the existing wide-load denitrification technologies are not suitable for addressing the startup phase of the unit's denitrification system. The industry currently faces a challenge in achieving continuous denitrification throughout the operational period of a 1000 MW tower furnace.

This study concentrates on the flue gas side and presents a range of continuous denitrification technologies that utilize rear-end heat input. In this section, we introduce and compare three preliminary design optimization options. These options include high-temperature flue gas direct mixing to enhance the temperature (Scheme (1)), bypass flue gas mixing to enhance the temperature through cooling (Scheme (2)), and high-temperature flue gas mixing with cold air to enhance the temperature (Scheme (3)).

4.1. Boundary Conditions

The design of a continuous flue gas denitrification system necessitates the comprehensive evaluation of denitrification operation conditions throughout different time periods, encompassing low-load operation as well as startup and shutdown phases. By taking into account the operational parameters of the Laizhou Power Plant during boiler operation and startup/shutdown periods and adhering to the boiler operation regulations with an

appropriate margin, the boundary conditions for the calculations have been established, as presented in Table 3.

Table 3. Boundary conditions for calculations.

Name	Unit	Startup			30% BMCR
Outlet temperature of the economizer cold flue gas	°C	150	180	210	280
Intermediate flue gas temperature at the outlet of the secondary reheater lower serpentube	°C	180	240	300	410
Total flue gas flow rate	Nm^3/h	1,000,000	1,000,000	1,000,000	1,392,728

(1) The boiler startup process involved selecting initial values for the SCR inlet flue gas temperature of 150 °C, 180 °C, and 210 °C, which corresponded to intermediate flue gas temperatures of 180 °C, 240 °C, and 300 °C at the outlet of the secondary reheater lower serpentube. The flue gas flow rate during this stage was 1,000,000 Nm^3/h, and the designed outlet temperature of the mixed flue gas from the hot air furnace was 650 °C. Upon heating the SCR inlet temperature to 300 °C, the primary air temperature could be set at 240 °C.

(2) During the load adjustment phase at 30% of BMCR, the SCR inlet flue gas temperature was approximately 280 °C with a flue gas flow rate of 1,392,728 Nm^3/h. The intermediate flue gas temperature at the outlet of the secondary reheater lower serpentube was set at 410 °C.

(3) The unit price of natural gas was USD 0.3/Nm^3, the unit price of diesel fuel was USD 820/t, and the unit price of standard coal was USD 150/t.

4.1.1. Scheme (1)

The system's conceptual diagram is presented in Figure 6, and the external structure of completed schematic design is shown in Figure S1. This approach entails the direct introduction of the hot flue gas produced by the hot air furnace into the primary flue, thereby raising the temperature of the SCR inlet flue gas to the permissible level for denitrification by means of heat and mass transfer. This ensures adherence to the operational specifications for denitrification.

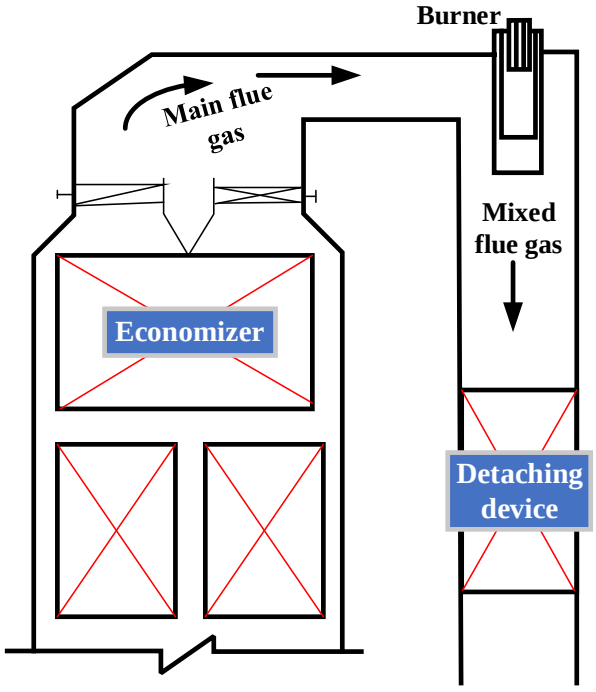

Figure 6. The schematic diagram of the high-temperature flue gas direct mixing system.

As shown in Table 4, the thermal calculations were conducted for four different operating conditions: the startup process with economizer outlet temperatures of 150 °C, 180 °C, and 210 °C, as well as low-load operation at 30% of the BMCR.

Table 4. Thermal calculation of high temperature flue gas direct mixing enhancement technology.

No	Items	Unit	Startup			30% BMCR
1	Natural gas heating value	kJ/Nm^3	35.88	35.88	35.88	35.88
2	Natural gas efficiency	/	0.99	0.99	0.99	0.99
3	Economizer outlet flue gas temperature	°C	150	180	210	280
4	Required flue gas temperature at the denitrification inlet	°C	300	300	300	300
5	Average specific heat of the flue gas	kJ/(m^3·K)	1.33	1.33	1.33	1.33
6	Average specific heat of the gas flue	kJ/(m^3·K)	1.377	1.377	1.377	1.377
7	Total flue gas volume	Nm^3/h	1,000,000	1,000,000	1,000,000	1,392,728
8	Required heat output from the hot air furnace	MW	64.70	51.76	38.82	12.01
9	Required natural gas quantity	Nm^3/h	6556.97	5245.57	3934.18	1217.61
10	Required gas quantity	kg/h	4683.55	3746.84	2810.13	870.00
11	Air–fuel ratio for natural gas	/	10	10	10	10
12	Combustion air flow rate	kg/h	46,835	37,468	28,101	8697
13	Combustion air temperature	°C	240	240	240	240
14	Combustion air density	kg/m^3	0.69	0.69	0.69	0.69
15	Actual combustion air flow rate	m^3/h	68,066	54,453	40,840	12,640
16	Design combustion air velocity	m/s	25	25	25	25
17	Combustion air duct inner diameter	mm	981	/	/	/
18	One-side combustion air duct inner diameter	mm	694	/	/	/
18	Increased flue gas losses	MW	18.42	16.75	12.94	/
19	Increased fuel costs	USD/h	183	350	365	143

The operating costs for the four different operating conditions are 6557 Nm^3/h, 5246 Nm^3/h, 3934 Nm^3/h, and 1218 Nm^3/h of natural gas consumption. During the startup phase, there is an additional flue gas heat loss ranging from 13 to 19 MW. In the low-load phase, the SCR inlet flue gas temperature increases by 20 °C. However, the impact on the flue gas temperature is negligible after the heat exchange process in the staged economizer and air preheater. It is important to note that a portion of the heat input at the rear end is absorbed by the staged economizer and air preheater, which can partially replace coal consumption. Based on estimations, the additional fuel cost after the operation of the system is expected to range from USD 137 to USD 343 per hour.

Impact assessment of auxiliary equipment: The calculated required flow rates of combustion air (primary hot air) were 13.0 kg/s, 10.4 kg/s, 7.8 kg/s, and 2.4 kg/s, confirming the adequacy of the primary air supply. Incorporating a primary air fan led to an approximate 200 kW increase in electrical consumption. The hot air furnace's flue gas and heat input contributed to an elevated flue gas temperature throughout the SCR system, resulting in an approximate 600 kW increase in electrical consumption for the induced draft fan that was attributable to these two factors.

The modification encompasses the hot air furnace body, the combustion air system, the front-end natural gas system, the hot air furnace outlet flue, and localized heat-resistant treatment within the main flue. The project intends to install four hot air furnaces, each with a capacity of 17,000 kW. To address the high temperature of the flue gas at the hot air furnace outlet, it is important to minimize the distance between the hot air furnace outlet and the main flue. The combustion air system is supplied from the primary air ducts located at the outlets of the hot air preheaters on both sides. These two branches, with an inner diameter of 800 mm, converge into a main pipe with an inner diameter of 1000 mm, which directs the airflow to the denitration system's entry platform. The gas piping for the front-end gas system is linked to the closest gas supply main pipe of the gas conversion system. The main pipe has a DN325 diameter, while the branch pipes have a DN100 diameter. The project's total estimated cost amounts to USD 239,000 due to the extensive range of equipment materials involved.

In this scheme, the hot air furnace outlet flue gas is directly introduced into the main flue without any cold air mixing, thereby presenting a risk of re-ignition when it comes into

contact with unburned particles within the main flue. If re-ignition occurs, an additional safety risk assessment is necessary that considers factors including particle burnout time and variations in the temperature field within the flue.

4.1.2. Scheme (2)

This scheme includes the extraction of flue gas from either the economizer inlet or further upstream locations. During boiler startup and shutdown phases, the extracted flue gas, acting as a cooling medium, is blended with high-temperature flue gas produced by the efficient hot air furnace. The mixture is subsequently directed to the economizer outlet at the designated temperature, effectively raising the inlet flue gas temperature to an optimal level for denitration. During periods of deep load adjustment, the high-temperature flue gas is directly delivered to the economizer outlet to increase the inlet flue gas temperature, facilitating denitration. Figure 7 illustrates the schematic diagram of the system. The extraction of flue gas is proposed at the central position (with a center elevation of 101.1 m) within the secondary low-temperature reheat serpentine tube arrangement (located behind the rear wall of the boiler) based on on-site investigations and comparisons. Flue gas extraction will be achieved by opening fins within the gaps of the water-cooled wall tubes.

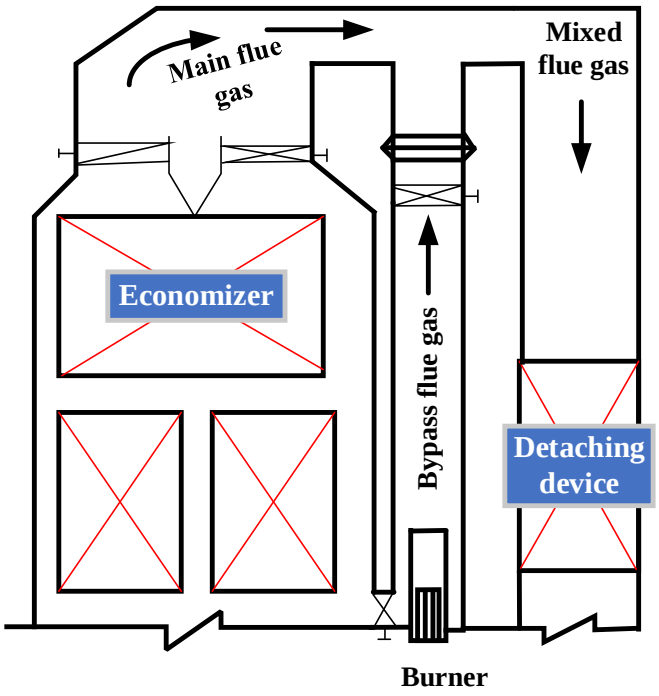

Figure 7. The schematic diagram of the high-temperature flue gas indirect mixing (sidestream flue gas mixing) system.

Table 5 presents the results of thermodynamic calculations for the high-temperature flue gas sidestream mixing for the temperature increase technique. The calculations were performed for four operating conditions: economizer outlet temperatures of 150 °C, 180 °C, 210 °C, and low-load operation (30% BMCR) during startup.

The operating costs were evaluated for different operational phases. During the startup phase, the costs associated with the bypass flue gas extraction were slightly lower compared to Scheme (1) due to a slightly higher temperature at the extraction point than at the economizer outlet. However, the difference was not significant. In the low-load phase, there were no additional operating costs as the hot air furnace was not in operation. However, during the medium to high-load phase, there was some leakage in the bypass damper, resulting in a approximately 5 °C increase in the SCR inlet flue gas temperature when accounting for a 3% leakage rate. This increase had no adverse effect on the safe

operation of the denitrification system under high and medium loads, and it had limited impact on the overall flue gas temperature.

Table 5. Thermodynamic calculation for high-temperature flue gas sidestream mixing.

No	Items	Unit	Startup			30% BMCR
1	Natural gas heating value	kJ/Nm^3	35.88	35.88	35.88	35.88
2	Natural gas efficiency	/	0.99	0.99	0.99	0.99
3	Economizer outlet flue gas temperature	°C	150	180	210	280
4	Temperature at the intermediate position of the secondary lower serpentube	°C	180	240	300	410
5	Temperature of the mixed flue gas at the hot air furnace outlet	°C	650	650	650	410
6	Required flue gas temperature at the denitrification inlet	°C	300	300	300	300
7	Average specific heat of the flue gas at 200 °C	kJ/(m^3·K)	1.33	1.33	1.33	1.33
8	Average specific heat of the flue gas at 400 °C	kJ/(m^3·K)	1.35	1.35	1.35	1.35
9	Average specific heat of the gas flue at 200 °C	kJ/(m^3·K)	1.377	1.377	1.377	1.377
10	Average specific heat of the gas flue at 400 °C	kJ/(m^3·K)	1.407	1.407	1.407	1.407
11	Total flue gas volume	Nm^3/h	1,000,000	1,000,000	1,000,000	1,392,728
12	Bypass flue gas volumetric flow rate	Nm^3/h	239,547	206,871	168,551	214,266
13	Actual bypass flue gas volume	m^3/h	397,491	388,735	353,771	536,057
14	Cold flue gas volume	Nm^3/h	760,453	793,129	831,449	1,178,462
15	Design flue gas velocity	m/s	15	15	15	15
16	Bypass flue gas extraction area	m^2	7.36	7.20	6.55	9.93
17	Required heat output from the hot air furnace	MW	61.60	46.40	32.28	0.00
18	Required natural gas quantity	Nm^3/h	6242.82	4703.00	3271.07	0.00
19	Required gas quantity	kg/h	4459.16	3359.28	2336.48	0
20	Air–fuel ratio for natural gas	/	10	10	10	10
21	Combustion air flow rate	kg/h	44,592	33,593	23,365	0
22	Combustion air temperature	°C	240	240	240	240
23	Combustion air density	kg/m^3	0.69	0.69	0.69	0.69
24	Actual combustion air flow rate	m^3/h	64,805	48,821	33,956	0
25	Bypass flue gas duct inner diameter	mm	3061	3028	2888	3555
26	Design combustion air velocity	m/s	25	25	25	25
27	Combustion air duct inner diameter	mm	957	/	/	/
28	Increased flue gas losses	MW	18.09	16.22	12.32	/
29	Increased fuel costs	USD/h	196	358	347	/

Auxiliary equipment impact assessment: The influence of auxiliary equipment was comparable to that of Scheme (1) during the startup phase. In the low-load phase, the absence of an external heat source resulted in a slightly lower flue gas volume that had to be handled by the induced draft fan, but the difference was not significant.

The retrofit scope encompasses the hot air furnace body, auxiliary air system, front-end natural gas system, and bypass flue gas duct system. Compared to Scheme (1), this approach necessitates the addition of a bypass flue gas duct system involving the installation of flue gas extraction points in the water-cooled walls and the introduction of a hot air furnace. This modification reduces the heat treatment workload at the rear end of the hot air furnace. The proposed arrangement involves the creation of a flue gas interface at the intermediate position (center elevation of 101.1 m) of the secondary lower serpentube on the rear wall of the boiler, achieved through the opening of finned tubes within the water-cooled walls. The initial calculation assumed a maximum open area of 10 m^2 for the water-cooled wall openings, and the feasibility of employing finned tube openings was confirmed through calculations conducted by the original boiler plant. Given the diverse range of equipment materials, the estimated total cost amounts to USD 328,000. During the subsequent stages of design and construction, particular attention should be given to implementing anti-wear treatments for the openings in the water-cooled walls and the upstream section of the lower serpentube.

4.1.3. Scheme (3)

This scheme utilizes the air preheater outlet to extract hot primary air or hot secondary air as a cooling medium. The extracted air is subsequently mixed with high-temperature

flue gas produced by the efficient hot air furnace and directed to the economizer outlet at the intended temperature. This process effectively elevates the inlet flue gas temperature for denitrification to a suitable level. Figure 8 illustrates the schematic diagram of the system. In this configuration, the hot primary air serves a dual purpose as both a combustion-supporting medium and a cooling medium.

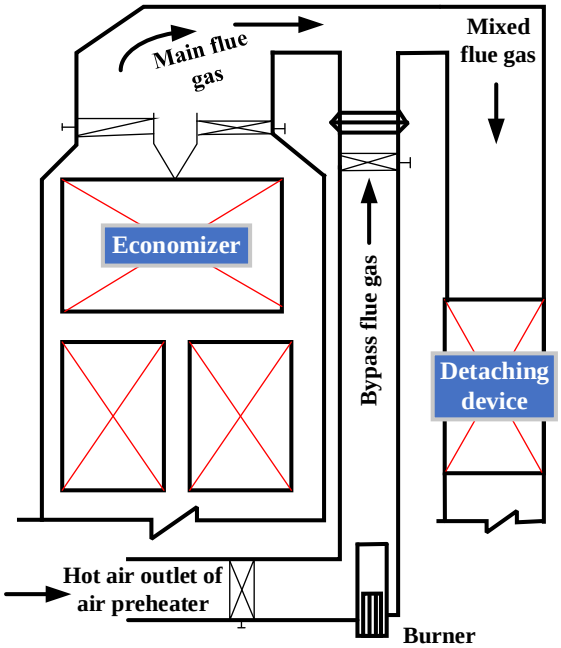

Figure 8. Schematic diagram of the high-temperature flue gas indirect mixing (cold air mixing with hot flue gas) system.

Table 6 displays the thermal calculation results for the high-temperature flue gas indirect mixing (cold air mixing with hot flue gas) technology. The calculations were conducted to evaluate four operating conditions: the startup process with economizer outlet temperatures of 150 °C, 180 °C, and 210 °C, as well as low-load operation at 30% of the BMCR.

Table 6. Thermal calculation results for high-temperature flue gas mixing with cold air for temperature enhancement.

No	Items	Unit	Startup			30% BMCR
1	Natural gas heating value	kJ/Nm^3	35.88	35.88	35.88	35.88
2	Natural gas efficiency	/	0.99	0.99	0.99	0.99
3	Economizer outlet flue gas temperature	°C	150	180	210	280
4	Primary hot air temperature	°C	240	240	240	240
5	Mixed flue gas temperature at the hot air furnace outlet	°C	650	650	650	650
6	Required flue gas temperature at the denitrification inlet	°C	300	300	300	300
7	Average specific heat of the flue gas at 200 °C	kJ/(m^3·K)	1.33	1.33	1.33	1.33
8	Average specific heat of the air at 400 °C	kJ/(m^3·K)	1.33	1.33	1.33	1.33
9	Average specific heat of the gas flue at 200 °C	kJ/(m^3·K)	1.377	1.377	1.377	1.377
10	Average specific heat of the gas flue at 400 °C	kJ/(m^3·K)	1.407	1.407	1.407	1.407
11	Total flue gas volume	Nm^3/h	1,000,000	1,000,000	1,000,000	1,392,728
12	Total hot air flow rate	Nm^3/h	417,635	334,108	250,581	55,685
13	Actual hot air flow rate	m^3/h	784,786	627,829	470,871	104,638
14	Design hot air velocity	m/s	25	25	25	25
15	Hot air duct inner diameter	mm	3.33	2.98	2.58	1.22
16	Required heat output from the hot air furnace	MW	72.05	57.64	43.23	9.61
17	Required natural gas quantity	Nm^3/h	7302.14	5841.71	4381.28	973.62
18	Increased flue gas losses	MW	24.53	21.62	16.59	/
19	Increased fuel costs	USD/h	361	496	468	114

Operating costs: The natural gas consumption for the four operating conditions is estimated to be 7302 Nm^3/h, 5842 Nm^3/h, 4381 Nm^3/h, and 974 Nm^3/h, respectively. During the startup phase, there is an additional flue gas heat loss of 16–25 MW, leading to an increased fuel cost of USD 360–495 per hour, which is approximately USD 205 per hour higher compared to the previous two schemes. During the low-load phase, the operating cost is approximately USD 135 per hour higher than that of Scheme (2).

Auxiliary equipment impact assessment: The required combustion air flow rates (primary hot air) are 149 kg/s, 120 kg/s, 90 kg/s, and 20 kg/s, respectively. Preliminary calculations indicate that the primary air supply is sufficient, with an additional power consumption of approximately 1000 kW for the primary air fan. Compared to the previous two schemes, this scheme significantly increases the flue gas volume, resulting in an additional power consumption of approximately 2000 kW for the induced draft fan.

The retrofit scope encompasses the hot air furnace body, the auxiliary air system, and the front-end natural gas system. In comparison to Scheme (1), this scheme requires a significant extraction of hot primary air for use as cooling air. Based on thermal calculations, the diameter of the main pipe for hot primary air is 3400 mm, while the diameter of the single-sided hot primary air pipe is 2400 mm. However, the significant elevation difference between the hot primary air pipeline and the SCR inlet platform results in higher pipeline costs and an inconvenient arrangement. Given the multitude of equipment materials, only the calculated total cost of USD 334,000 is provided here.

4.2. Comparative Evaluation of Continuous Denitrification Technologies

4.2.1. Scheme (1)

This approach offers the benefits of a simple system, low investment, and cost-effective operation. The research findings indicate that coal combustion during the unit's ignition phase is suboptimal, leading to a volatile matter content in the fly ash of up to 13.20%. Empirical formulas suggest that the lowest ignition temperature for the resulting dust cloud is around 740 °C. By employing high-temperature flue gas direct mixing for temperature enhancement, flue gas temperatures as high as 2000 °C can be achieved. However, during the initial stages, uneven mixing and localized high temperatures may occur, potentially causing secondary combustion and posing safety hazards to the flue system. Moreover, frequent start–stop cycles of the burner during low-load operation result in increased fuel costs and adversely affect equipment longevity.

Furthermore, the introduction of high-temperature flue gas into the main flue necessitates the use of refractory materials throughout the entire flue. This construction work is estimated to cover an area of approximately 2500 m^2, with a thickness of about 20 mm. Additionally, a thorough evaluation and reinforcement of the existing flue supports are required. Considering safety considerations, this feasibility study does not recommend adopting this particular technological approach.

4.2.2. Scheme (2)

This approach offers several advantages:

The heat generated from fuel combustion is fully utilized to raise the flue gas temperature in the main flue, resulting in minimal fuel consumption for the heating system. The extracted high-temperature flue gas temperature is higher than the economizer outlet flue gas temperature, leading to potentially lower natural gas consumption during various ignition stages compared to Scheme (1).

During low-load operation, there is no need to operate the hot air furnace. The denitrification requirements can be met through internal heat transfer within the boiler, eliminating the need for frequent start–stop cycles of the burner and reducing fuel costs during the low-load phase.

By adjusting the damper opening at the economizer outlet to increase the resistance in the main flue, the proportion of main and bypass flue gases can be distributed without the need for additional circulating fans. This approach avoids safety risks associated with

installing rotating machinery at elevated locations and reduces the operating cost of the circulating fans.

Additionally, based on thermal calculations and assessments conducted by the original boiler manufacturer, the opening of fins in the water-cooled walls meets design requirements without compromising boiler safety. Although potential issues with damper door deformation and sticking may arise, these concerns can be effectively addressed through strict control measures during the design, construction, and maintenance processes. Considering both technical functionality and economic feasibility, it is recommended to adopt this retrofitting technology.

4.2.3. Scheme (3)

This approach offers the following advantages:

The heat generated from fuel combustion is fully utilized to raise the temperature of the flue gas in the main duct, resulting in minimal fuel consumption for the heating system. As the extracted high-temperature flue gas is hotter than the economizer outlet flue gas, the natural gas consumption during the ignition stages is even lower than in Scheme (1).

The low dust content in the hot air eliminates concerns regarding damper sticking.

Compared to the cold air mixing technology, this system operates with lower overall costs.

However, in comparison to Scheme (2), several shortcomings exist:

Due to the temperature difference in heat exchange between the hot air at the air preheater outlet and the flue gas at the air preheater inlet as well as additional heat exchange with the staged economizer the operating costs of the hot air furnace system are relatively higher. The thermal calculations show that the natural gas consumption during the ignition stages is approximately 1000 Nm^3/h higher than in Scheme (2), necessitating larger dimensions for the hot air furnace.

During low-load operation, if the inlet flue gas temperature for denitrification cannot reach the design value, the hot air furnace needs to be activated for heating, leading to increased fuel costs. Under the same operating conditions of 30% BMCR, it consumes an additional 1000 Nm^3/h of natural gas compared to Scheme (2). Moreover, the frequent start–stop cycles of the burner can affect its service life. Considering the normalization of low-load operation from both an economic and equipment-reliability standpoint, this approach is not optimal.

The introduction of hot air increases the total volume of flue gas flowing through the hot air furnace, necessitating larger furnace and outlet pipeline sizes.

The addition of hot air increases the flue gas volume at the air preheater outlet, resulting in increased flue gas heat loss. Additionally, the power consumption of the primary air fan and induced draft fan increases significantly.

Considering the technical and economic aspects, this feasibility study does not recommend adopting this technological approach.

5. Conclusions

The existing wide-load denitrification technologies are not suitable for addressing the startup phase of the unit's denitrification system, which poses a challenge for achieving continuous denitrification throughout the operational period. Three potential retrofitting schemes were analyzed:

- Scheme (1) (direct mixing of high-temperature flue gas): This scheme is simple and cost-effective, but it presents safety hazards and requires extensive refractory materials and reinforcement of the flue supports. It is not recommended due to safety concerns.
- Scheme (2) (bypass flue gas mixing for temperature enhancement): This scheme offers advantages such as efficient heat utilization, reduced fuel consumption, and feasibility. It can meet denitrification requirements through internal heat transfer and controlled opening of fins in water-cooled walls. It is the preferred retrofitting technology for achieving continuous denitrification.

- Scheme (3) (indirect mixing of hot flue gas with cold air): This scheme has higher operating costs, larger dimensions, and increased flue gas heat loss compared to Scheme (2). It is not recommended due to higher costs and less favorable operating conditions.

Based on the comparative evaluation, Scheme (2) is recommended as the preferred retrofitting technology for achieving continuous denitrification. It balances technical functionality, economic feasibility, and safety considerations.

This study provides detailed thermodynamic calculations, operating costs, auxiliary equipment impact assessment, retrofit scope, and estimated total costs for each scheme, which can aid in decision making for the denitrification system retrofit. In conclusion, Scheme (2), utilizing bypass flue gas mixing for temperature enhancement, is the recommended approach to achieve continuous denitrification in the studied coal-fired power plant, considering its technical viability, cost-effectiveness, and safety aspects.

Supplementary Materials: The following supporting information can be downloaded at: https://www.mdpi.com/article/10.3390/pr12010056/s1, Figure S1: The external structure of completed schematic design.

Author Contributions: Conceptualization, J.H.; Methodology, D.G.; Software, Y.Z.; Validation, X.K. and H.X.; Formal analysis, X.Y. and X.G.; Investigation, X.Y.; Data curation, J.H.; Writing—original draft, X.Y.; Writing—review & editing, C.Z.; Visualization, X.K. All authors have read and agreed to the published version of the manuscript.

Funding: This research was supported by the National Key R&D Plan of China (No. 2022YFB4100805) and the Technology Project of China Huadian Group Co., Ltd. (No. CHDKJ21-01-41).

Data Availability Statement: Data are contained within the article.

Conflicts of Interest: Author Xinrong Yan, Jianle He, Dong Guo and Yang Zhang were employed by the company Huadian Electric Power Research Institute Co., Ltd. The remaining authors declare that the research was conducted in the absence of any commercial or financial relationships that could be construed as a potential conflict of interest. The authors declare that this study received funding from China Huadian Group Co., Ltd. The funder was not involved in the study design, collection, analysis, interpretation of data, the writing of this article or the decision to submit it for publication.

References

1. Yang, S.; Yang, D.; Shi, W.; Deng, C.; Chen, C.; Feng, S. Global evaluation of carbon neutrality and peak carbon dioxide emissions: Current challenges and future outlook. *Environ. Sci. Pollut. Res.* **2022**, *30*, 81725–81744. [CrossRef]
2. Wang, Y.; Guo, C.-H.; Chen, X.-J.; Jia, L.-Q.; Guo, X.-N.; Chen, R.-S.; Zhang, M.-S.; Chen, Z.-Y.; Wang, H.-D. Carbon peak and carbon neutrality in China: Goals, implementation path and prospects. *China Geol.* **2021**, *4*, 720–746. [CrossRef]
3. Zhao, X.; Ma, X.; Chen, B.; Shang, Y.; Song, M. Challenges toward carbon neutrality in China: Strategies and countermeasures. *Resour. Conserv. Recycl.* **2022**, *176*, 105959. [CrossRef]
4. Liu, Z.; Deng, Z.; He, G.; Wang, H.; Zhang, X.; Lin, J.; Qi, Y.; Liang, X. Challenges and opportunities for carbon neutrality in China. *Nat. Rev. Earth Environ.* **2022**, *3*, 141–155. [CrossRef]
5. Wei, Y.-M.; Chen, K.; Kang, J.-N.; Chen, W.; Wang, X.-Y.; Zhang, X. Policy and management of carbon peaking and carbon neutrality: A literature review. *Engineering* **2022**, *14*, 52–63. [CrossRef]
6. Sun, L.-L.; Cui, H.-J.; Ge, Q.-S. Will China achieve its 2060 carbon neutral commitment from the provincial perspective? *Adv. Clim. Chang. Res.* **2022**, *13*, 169–178. [CrossRef]
7. Yang, Y.; Guo, X.; Wang, N. Power generation from pulverized coal in China. *Energy* **2010**, *35*, 4336–4348. [CrossRef]
8. Yuan, J.; Na, C.; Lei, Q.; Xiong, M.; Guo, J.; Hu, Z. Coal use for power generation in China. *Resour. Conserv. Recycl.* **2018**, *129*, 443–453. [CrossRef]
9. Hepburn, C.; Qi, Y.; Stern, N.; Ward, B.; Xie, C.; Zenghelis, D. Towards carbon neutrality and China's 14th Five-Year Plan: Clean energy transition, sustainable urban development, and investment priorities. *Environ. Sci. Ecotechnol.* **2021**, *8*, 100130. [CrossRef]
10. Mohsin, M.; Hanif, I.; Taghizadeh-Hesary, F.; Abbas, Q.; Iqbal, W. Nexus between energy efficiency and electricity reforms: A DEA-based way forward for clean power development. *Energy Policy* **2021**, *149*, 112052. [CrossRef]
11. Zeng, M.; Yang, Y.; Wang, L.; Sun, J. The power industry reform in China 2015: Policies, evaluations and solutions. *Renew. Sust. Energ. Rev.* **2016**, *57*, 94–110. [CrossRef]
12. Zou, C.; Zhao, Q.; Zhang, G.; Xiong, B. Energy revolution: From a fossil energy era to a new energy era. *Nat. Gas Ind. B* **2016**, *3*, 1–11. [CrossRef]

13. Pradhan, B.K.; Ghosh, J. A computable general equilibrium (CGE) assessment of technological progress and carbon pricing in India's green energy transition via furthering its renewable capacity. *Energy Econ.* **2022**, *106*, 105788. [CrossRef]
14. Jie, D.; Xu, X.; Guo, F. The future of coal supply in China based on non-fossil energy development and carbon price strategies. *Energy* **2021**, *220*, 119644. [CrossRef]
15. Pehl, M.; Arvesen, A.; Humpenöder, F.; Popp, A.; Hertwich, E.G.; Luderer, G. Understanding future emissions from low-carbon power systems by integration of life-cycle assessment and integrated energy modelling. *Nat. Energy* **2017**, *2*, 939–945. [CrossRef]
16. Wang, J.; Zhang, S.; Huo, J.; Zhou, Y.; Li, L.; Han, T. Dispatch optimization of thermal power unit flexibility transformation under the deep peak shaving demand based on invasive weed optimization. *J. Clean. Prod.* **2021**, *315*, 128047. [CrossRef]
17. Feng, Z.-K.; Niu, W.-J.; Wang, W.-C.; Zhou, J.-Z.; Cheng, C.-T. A mixed integer linear programming model for unit commitment of thermal plants with peak shaving operation aspect in regional power grid lack of flexible hydropower energy. *Energy* **2019**, *175*, 618–629. [CrossRef]
18. Dowell, N.M.; Staffell, I. The role of flexible CCS in the UK's future energy system. *Int. J. Greenh. Gas Control* **2016**, *48*, 327–344. [CrossRef]
19. Xi, X.; Zhang, W.; Zhu, Y.; Zhang, J.; Yuan, J. Wind integration cost in China: A production simulation approach and case study. *Sustain. Energy Technol. Assess.* **2022**, *51*, 101985. [CrossRef]
20. Vargas-Ferrer, P.; Álvarez-Miranda, E.; Tenreiro, C.; Jalil-Vega, F. Integration of high levels of electrolytic hydrogen production: Impact on power systems planning. *J. Clean. Prod.* **2023**, *409*, 137110. [CrossRef]
21. Qin, P.; Tan, X.; Huang, Y.; Pan, M.; Ouyang, T. Two-stage robust optimal scheduling framework applied for microgrids: Combined energy recovery and forecast. *Renew. Energ.* **2023**, *214*, 290–306. [CrossRef]
22. Xie, G.; Gu, C.; Cao, P.; Zhang, P.; Duan, S.; She, J.; Liu, X.; Xin, S.; Guo, R.; Du, J. Research on the effect of the flue gas recirculation on the combustion and operating economy of circulating fluidized bed boiler. *IOP Conf. Ser. Earth Environ. Sci.* **2023**, *1171*, 012005. [CrossRef]
23. Taler, J.; Trojan, M.; Dzierwa, P.; Kaczmarski, K.; Węglowski, B.; Taler, D.; Zima, W.; Grądziel, S.; Ocłoń, P.; Sobota, T. The flexible boiler operation in a wide range of load changes with considering the strength and environmental restrictions. *Energy* **2023**, *263*, 125745. [CrossRef]
24. Shen, X.; Li, J.; Jia, L.; Wang, Y.; Guo, B.; Qiao, X.; Yang, H.; Zhang, M.; Jin, Y. Numerical simulation of NO and SO2 emission dynamic characteristics during thermal start-up of CFB boiler. *Particul. Sci. Technnol.* **2022**, *41*, 53–63. [CrossRef]
25. Guo, S.; Liu, G.; Liu, S. Driving factors of NOX emission reduction in China's power industry: Based on LMDI decomposition model. *Environ. Sci. Pollut. Res.* **2023**, *30*, 51042–51060. [CrossRef]
26. Sun, K.; Ao, T.; Liu, X.; Liu, L.; Liang, Z. Experiment and Numerical Simulation Study of Low-nitrogen Combustion Technology inside Small Gas Boiler. *J. Energy Resour. Technol.* **2023**, *145*, 104501. [CrossRef]
27. Damiri, D.; Damanhuri, D. Comparison of mixed fuel coal and palm shells on operation 135 MW circulating fluidized bed boiler steam powerplant. *AIP Conf. Proc.* **2023**, *2646*, 050039.
28. Rahman, M.N.; Yusup, S.; Fui, B.C.L.; Shariff, I.; Quitain, A.T. Oil Palm Wastes Co-firing in an Opposed Firing 500 MW Utility Boiler: A Numerical Analysis. *CFD Lett.* **2023**, *15*, 139–152. [CrossRef]
29. Li, X.; Wang, H.; Wang, S. Study on optimization and adjustment of high sodium coal pulverization system for 660 MW boiler. In Proceedings of the International Conference on Mechatronics Engineering and Artificial Intelligence (MEAI 2022), Changsha, China, 11–13 November 2022; SPIE: Bellingham, WA, USA, 2023; pp. 333–339.
30. Nikparto, A.; Sardar, A.; Herrin, D. Prediction of Combustion Driven Oscillation in a Residential Ultra-Low NOx Gas Furnace Product Using a Positive Feedback Stability Model. In *INTER-NOISE and NOISE-CON Congress and Conference Proceedings*; Institute of Noise Control Engineering: Washington, DC, USA, 2023; pp. 290–299.
31. Ding, X.; Feng, C.; Yu, P.; Li, K.; Chen, X. Gradient boosting decision tree in the prediction of NOx emission of waste incineration. *Energy* **2023**, *264*, 126174. [CrossRef]